CHALMERS
UNIVERSITY OF TECHNOLOGY

Wideband OMT for the 210-373 GHz Band With Built-in 90? Waveguide Twist

Wideband OMT for the 210-373 GHz Band with Built-in 90º Waveguide Twist

Igor Lapkin, Cristian López, Denis Meledin, Leif Helldner, Mathias Fredrixon, Alexey Pavolotsky, Sven-Erik Ferm, Vincent Desmaris, Victor Belitsky, *Senior Member IEEE*

***Abstract*—We present the design of a wideband orthomode transducer, OMT, that aims for the frequency band 210 - 373 GHz. The OMT employs a modified Bøifot layout and is optimized to fit into the tight spatial constraints, e.g., of the ALMA cartridge. The OMT layout harmonizes the receiver cartridge components for both polarizations by allowing use of the same configuration and components in both polarization chains because of the OMT outputs' colinear positioning. The OMT features a built-in novel broadband 90-degree waveguide twist, which minimizes the insertion RF loss by removing the H-split waveguide while eases receiver components integration with the 2SB mixers in the ALMA cartridge. The manufactured OMT was characterized by direct measurements with a VNA employing frequency extension modules. The waveguide adapters were used accommodating the OMT waveguide ports having dimensions 760x760 µm for the input port and 380x760 µm for the output ports to the VNA extension modules. The OMT demonstrated the cross-poll better than - 25dB across 95% of the frequency band, the output reflections better than 15 dB and the RF insertion loss better than 0.8 dB.**

***Index Terms* — Dual-polarization receivers, orthomode transducer, waveguides, ALMA receiver cartridge**

I. INTRODUCTION

An orthomode transducer, OMT, is a polarization diplexer that allows to separate the polarization components of an incoming signal. A typical place for such diplexer is between the feed, e.g., a corrugated horn, and the first stage of a dual-polarization receiver, e.g., a mixer. Consequently, the input port of an OMT should allow propagation of both orthogonal linear polarizations and the OMT insertion RF loss should be minimized as the loss directly affects the receiver noise performance. In this paper, we focus on radio astronomy applications however suggested OMT could be used for any relevant application. A few derivatives of the Bøifot OMT layout [1] are currently used in the ALMA observatory [2] Band 3, 4, 5, 6, 8 receiver channels providing superior beam squint performance on sky with the single feed for both polarizations as compared to the receivers using polarization grids and thus employing individual feeds for each polarization that needs careful mechanical alignment, Fig 1.

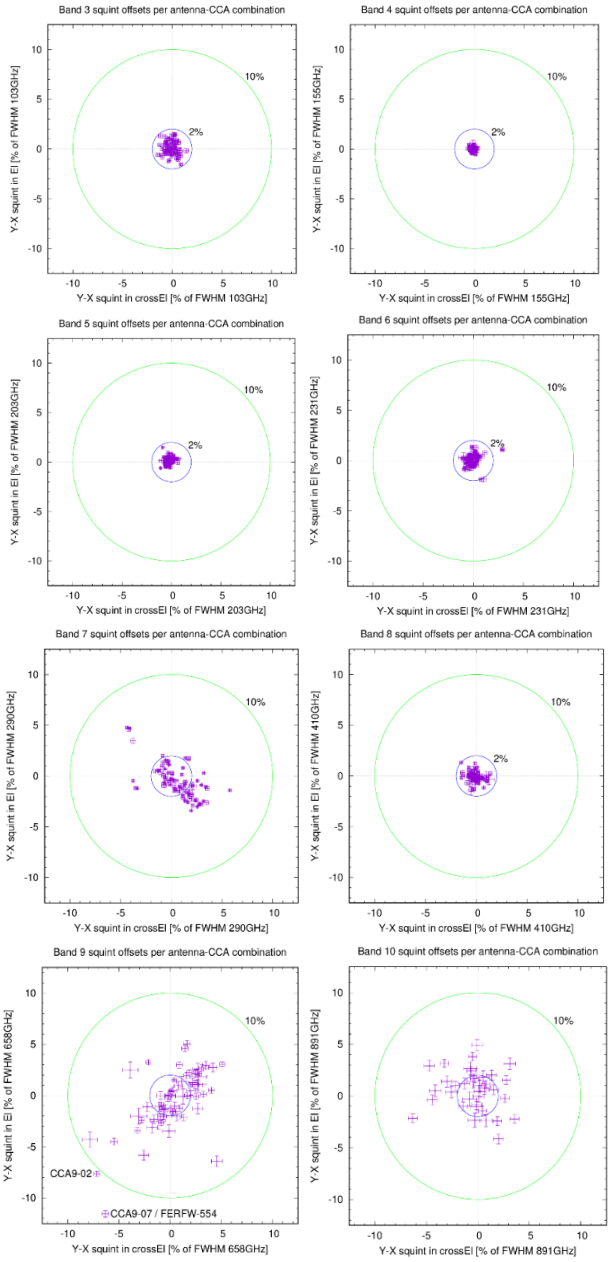

Fig. 1. On-sky Y-X polarization beam squint in cross-elevation vs. elevation coordinates in units of the beam FWHM at the

This paragraph of the first footnote will contain the date on which you submitted your paper for review, which is populated by IEEE. This work was supported by the Onsala Space Observatory, Swedish National Facility for Radio Astronomy, and by the European Southern Observatory via Collaboration Agreement No. 94468/20/103859/HNE. *Corresponding author: Victor Belitsky, victor.belitsky@chalmers.se.*

All authors are with the Group for Advanced Receiver Development, Onsala Space Observatory, Department of Space, Earth and Environmental Sciences, Chalmers University of Technology, Gothenburg, SE-41296, Sweden. E-mail to all authors is name.surname@chalmers.se.

Color versions of one or more of the figures in this article are available online at http://ieeexplore.ieee.org

observing frequency for ALMA Bands 3 to 10. Multiple measurements have been averaged per antenna-CCA combination when possible. The 10% specification limit is shown (green circle), in addition to a threshold of 2% which all existing single-horn receivers (Bands 3, 4, 5, 6, 8) could comply with and which may be a practical future goal. This figure corresponds to Figure 8 in [3].

Therefore, the implementation of an OMT in the next generation of ALMA receivers, including ALMA Band 7, 9 and 10, is a desirable option. Up to the date, several OMT designs are known but the OMT originating from the Bøifot layout has proven to provide very competitive performance in terms of the insertion RF loss, reflections and cross-polarization. Based on that experience and having heritage of delivering ALMA Band 5 receivers, we focus this manuscript on the wideband derivative of the Bøifot OMT layout. In Chapter V, we present a comparison table that includes different OMTs and its performances.

The ALMA receiver cartridges provide a very confined space for placing receiver components especially considering all cold optics with bigger mirrors, particularly for lower frequency bands with all-cold optics, e.g., ALMA Band 5 [4] and even Band 6. The original Bøifot OMT's T-layout precludes using the same components and arrangement of the receivers for both polarizations that would be a disadvantage for, e.g., ALMA receiver cartridge production. However, this difficulty could be circumvented by slightly more complex OMT configuration, which include additional split of the block and 90-degree H-plane turns of the waveguides at the Y-junction branch as in ALMA Band 5 OMT [5]. However, this solution has a drawback of featuring an extended H-split waveguide for one polarization that may result in an RF leak and correspondingly an increased insertion RF loss. This is especially true for an OMT at higher frequencies, e.g., targeted OMT RF bandwidth 210 - 373 GHz where the waveguide dimensions are substantially smaller and require even higher accuracy for fabrication.

In order to avoid the unwanted H-split and risk of increasing the insertion RF loss, we introduce an integrated 90-degree wideband waveguide twist with novel design and placed close to the OMT polarization splitting junction. This allows to co-align OMT output waveguides and avoid using external 90 - degree twist as in [5, 6]. By harmonizing the OMT outputs, we allow using the same receiver components and layout for both polarizations.

II. Wideband Waveguide 90-degree Twist

In general, an OMT built using split-block technique with co-aligned outputs cannot avoid employing an unwanted H-split inherently as the polarization splitting junction handles 2 orthogonal polarizations. As we discussed above, integrated 90-degree waveguide twist placed closer to the polarization splitting junction helps to minimize the length of the waveguides with H-split.

In order to keep the length of the waveguides inside OMT to possible minimum and thus introduce minimum insertion RF loss, a compact 90-degree waveguide twist should be introduced for integration inside the OMT, e.g., as described in [7, 8, 9, 10]. The twist has to be compatible with split-block fabrication technique intended to fabricate the OMT. Another obvious feature of the twist is that it provides 56% of the fractional RF band and deliver 210 - 373 GHz operational bandwidth.

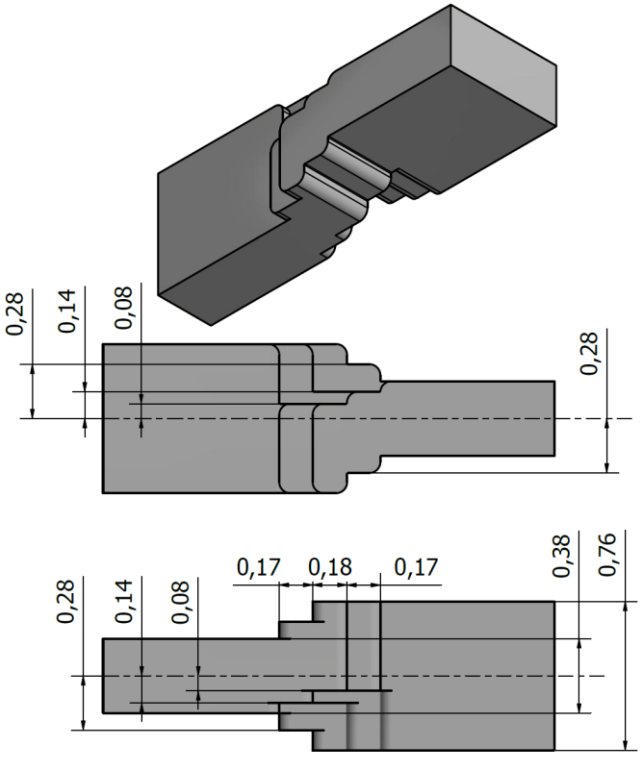

Fig. 2. Novel 3-step waveguide 90-degree twist. *Top:* 3D model of twist that uses the layout similar to the twist [9] in the middle section with the two adjacent twist sections resembling the layout of the twist presented in [11]. The model has filleted corners, R=50 µm, to address constrains of the milling (Ø90 µm milling tool). Waveguide dimensions are 380 x 760 µm. The split goes in the middle of the broad wall of the waveguide at the left side and continues in the middle of the narrow wall of the waveguide at the right. The two projections of the twist depicted below the 3D model have all necessary dimensions.

The required bandwidth could be provided by the twist suggested in [8], however its design is hardly suitable for the split-block fabrication. The twists suggested in [9, 10] could be accommodated to fabrication using split-block technique but do not provide the required RF bandwidth. Following these conclusions, we introduce a novel twist which uses modified layout of the one presented in [9] in a multi-step design in order to extend the RF band. Fig. 2 illustrates the initial design with the twist similar to [9] in the central position while the two adjacent peripheral steps use the twist shape similar to presented in [11]. Fig. 2 displays the resulting HFSS model in which changes in the initial layout address the manufacturing approach and use of the miller by applying fillet to the sharp 90-degree corners of the initial twist layout.

The final design of the three-step twist was optimized using HFSS simulations and realistic constrains of the fabrication using precision CNC miller. The results of the optimized twists HFSS simulations are presented in Fig. 3.

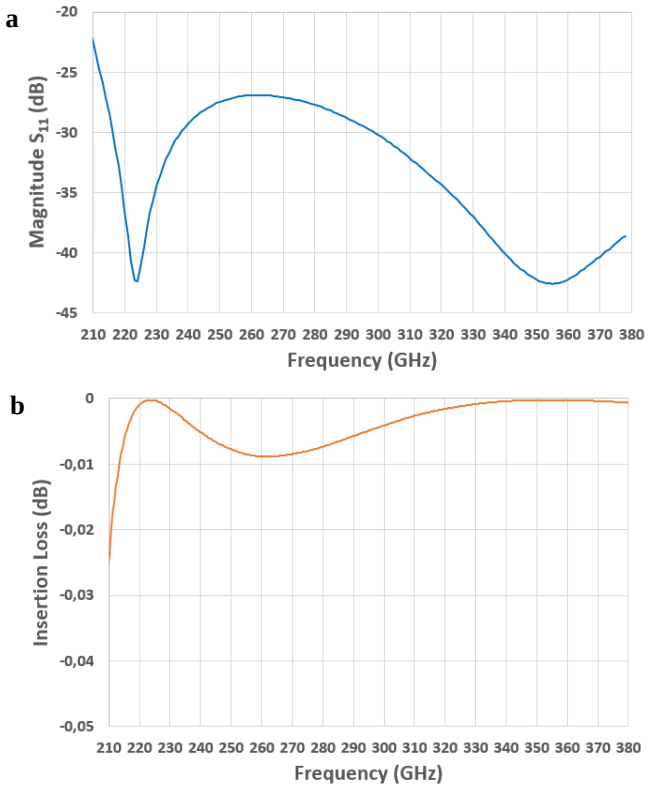

Fig. 3. HFSS simulation results of the twist 3-step structure. *Fig. 3a* displays the return loss and *Fig. 3b* presents the insertion RF loss (simulations were performed for PEC).

In order to experimentally verify the performance of the designed twist, we fabricated back-to-back two twists in a block as depicted in Fig. 4.

The block was made from aluminum alloy using split-block approach with the feeding waveguides split in the middle of the broad wall and only short waveguide connecting the two twists has split in the middle of the short wall. This way, we minimize effect of the "wrong" split on the measurement results.

Fig. 4. Photos of the block with back-to-back twists. The block manufactured from aluminum alloy. Waveguide dimensions are 380 x 760 µm.

In order to calibrate out the insertion RF loss of the waveguides, we fabricated a reference block with the straight waveguide length less by 1.77 mm, the length between the starting and ending points of the two twists, and which insertion RF loss were measured and subtracted from the block insertion RF loss that contains the twists.

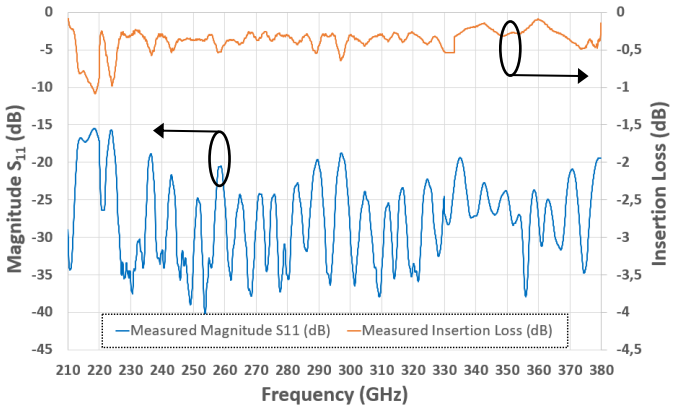

Fig. 5. Measurement results of the back-to-back twists: the return loss per one twist (blue line) and the insertion RF loss (orange line) per one twist using additional measurement data of the block without the twists to de-embed the performance of the twist.

The test structure was made of aluminum alloy that has about 3 times less conductivity than Gold. The measurements of the insertion RF loss do not remove the RF loss in the small piece of the waveguide between the two twists. Furthermore, it is very difficult to achieve very high repeatability of the waveguide performance manufactured by milling, in our case a difference in the RF insertion loss between the waveguide with and without twists of 0.01 dB/mm would produce an error of about 0.23 dB in the estimation of the insertion RF loss. Consequently, the measurement of the back-to-back twists was intended to demonstrate the absence of resonances and extremely flat and wideband performance of the twist while the insertion RF loss data is indicative. The back-to-back twist manufactured block was characterized by using a Keysight PNA-X VNA and WR5.1, WR 3.4 and WR2.2 frequency extension modules from VDI. The measurement results are presented in Fig. 5.

III. OMT Layout & Simulations

The OMT design largely follows the one successfully used in the ALMA Band 5 receiver [5]. Fig. 6 depicts the HFSS 3D final model of the OMT.

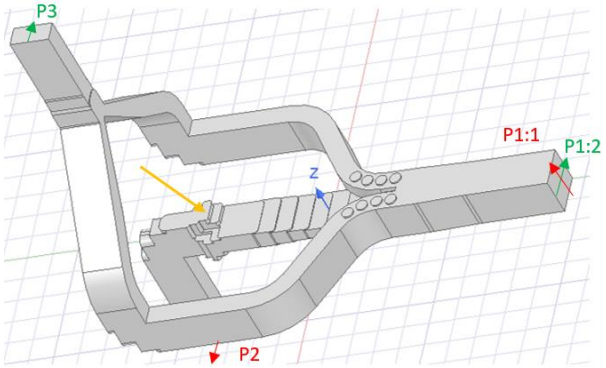

Fig. 6. HFSS optimized OMT 3D model. Yellow arrow points on the built-in twist. Polarization split illustrated by color-coded port denotations.

In order to achieve substantially broader fractional bandwidth, 210-373 GHz or 56% of the center frequency and to have a better control over the internal matching, additional elements were added to the polarization splitting junction, in particular, a multi-step transformer was added to the direct output of the polarization splitting junction and multiple circular recesses to Y-junction branch of the polarization splitting junction. During the OMT HFSS simulation, we needed additional "tuner" to extend and equalize the performance over the targeted RF band 210-373 GHz. Using different elements of the OMT and employing heuristic approach, it was found that such circular recesses provide convenient "tuning tool". **In particular, by varying the sizes and number of recesses and their spacing, we could gently modulate the *effective* width of the waveguides in the OMT polarization splitting junction, Fig. 6, for those leading towards the waveguide Y-junction. The changes in the *effective* waveguide width have a very confined geometry and are interleaved by standard rectangular waveguide sections. Consequently, this does not create any longer oversized waveguide with a risk of having trapped modes and facilitates tuning the OMT to the desirable bandwidth and performance level.**

During design phase, all major waveguide components of the OMT, the polarization splitting junction, the Y-junction, the twist and H-turns were HFSS simulated and optimized separately with the goal of having input/output reflection loss well below -20 dB. Thereafter, the complete HFSS OMT model was assembled by combining these partial models and the optimization procedure was re-run for the complete OMT model. The results of the HFSS simulations are presented in Fig. 7.

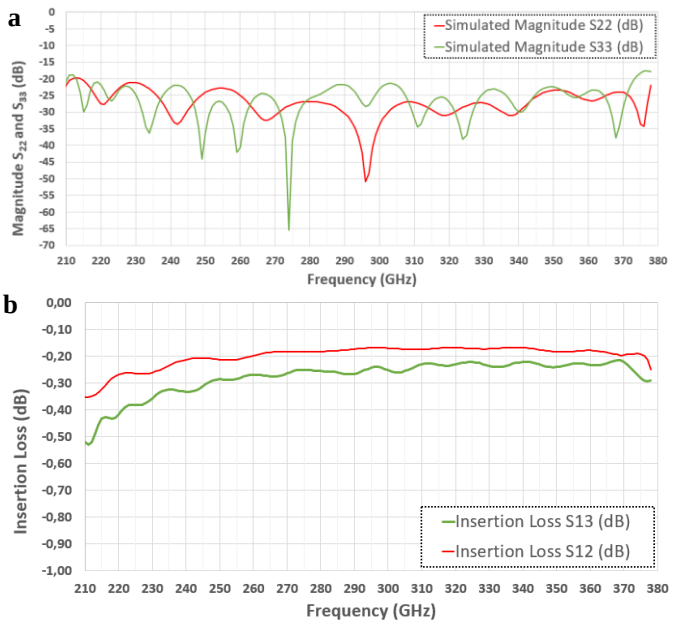

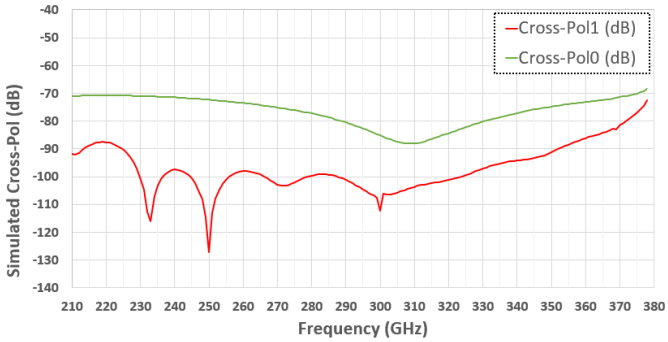

Fig. 7. HFSS simulation results of the OMT. *Fig. 7a* displays the return loss at the waveguides' outputs. *Fig. 7b* presents the insertion RF loss for each polarization (for electroplated gold assigned as material for the OMT in HFSS). *Fig. 7c* presents the cross-pol simulation results.

The HFSS simulations for Pol. 0 correspond to the port P1:2 & P3 and the Pol. 1 correspond to P1:1 & P2 in Fig. 6. In the HFSS simulation results that are presented in Fig.7, it was assumed perfect geometry and as such Fig. 7 displays theoretical limit / ultimate accuracy of the simulations software and yet demonstrates potential of the presented here OMT design. The HFSS OMT simulations also included tolerance analysis of the final design in order to verify that the OMT has sufficient margins to be produced in the in-house workshop. In particular, we introduced shifts between the 3 blocks constituting the OMT. The simulations have shown low sensitivity to the offset up to 10 µm of the split in the plain of P2 – P3, Fig. 6, but stronger sensitivity in the split plain of P1:2 which goes through the polarization splitting junction and shows the performance changes with offset above 5 µm. Yet, the tolerance analysis confirmed that the designed OMT is fully doable using our CNC Kern™ Evo milling machine with the positional accuracy of ±0.5 µm. The geometry of the produced blocks was controlled by using 3D Optical Profiler System ZeGage™ by Zygo Corporation to ensure compliance with the designed parameters.

IV. OMT Fabrication & Characterization

The twist is placed at the polarization splitting junction output for polarization P1:1 as depicted in Fig. 6. The OMT is an assembly of 3 blocks: two blocks with split in the middle of the square input waveguide aligned with the polarization P1:2, Fig. 6. Thus, only the waveguide multi-step transformer section (P2) has H-split. Another split goes between the former two-block assembly comprising the square input waveguide and the polarization splitting junction, and the third block with the plane of the split in the middle of the OMT output waveguides, the plane corresponding to P2, P3 as in Fig. 6.

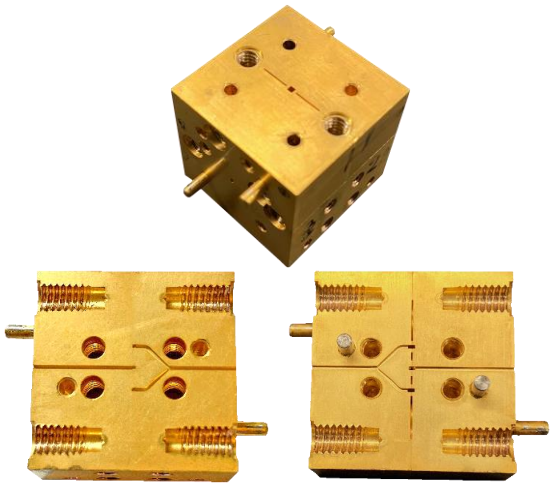

Fig. 8. Manufactured OMT. Pictures show assembled OMT with the square input waveguide, top photo. Solid part of the second split (left) and the split part that containing the polarization splitting junction, right. In this split all waveguides are divided in the middle of the broad wall (non-radiating split) and are co-aligned. The OMT is manufactured from Tellurium copper and gold-plated.

The OMT was manufactured in our in-house workshop using precision CNC milling machine. Tellurium copper was used for manufacturing with following electro-plating with 0.5 µm thick Gold. Fig. 8 shows the manufactured OMT. The OMT was characterized using the same Keysight PNA-X VNA and frequency extension modules WR5.1, WR3.4 and WR2.2. The OMT characterization results are depicted in Fig. 10.

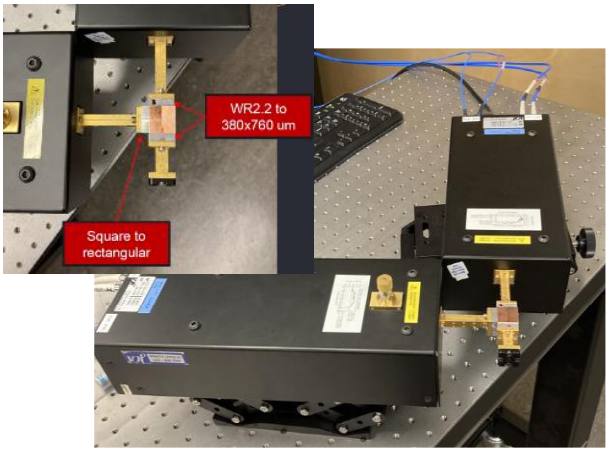

Fig. 9. The OMT measurement setup. The insert shows use of the adapters and transitions needed for the measurements. The idle port is terminated by matched load during the measurements.

Because the OMT uses custom-sizes of the waveguides 380 x 760 µm and 760 x 760 µm, the measurements required adapters for rectangular waveguides and transitions rectangular-to-square from the waveguides of the VNA frequency extension modules as depicted in Fig. 9 insert.

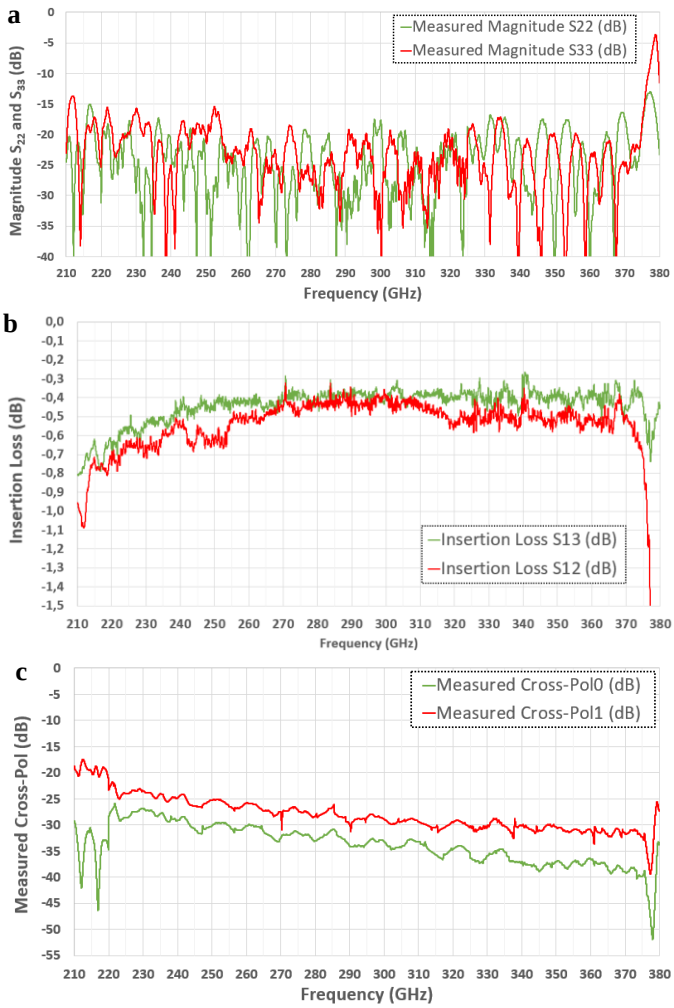

Fig. 10. Measured performance of the OMT. *Fig. 10a* displays the return loss at the OMT waveguide's outputs. *Fig. 10b* presents the insertion RF loss for each polarization. *Fig. 10c* shows the cross-pol measurement results. As mentioned above, Pol. 0 corresponds to the port P1:2 & P3 and the Pol. 1 corresponds to P1:1 & P2 as in Fig. 6.

While the insertion RF loss in the adapters and transitions could be calibrated out in the back-to-back configurations, the reflection could be only measured excluding the adapters as the standard calibration kits allowed calibrate the ports directly at the frequency extension modules. Additional factor of measurements' inaccuracy was the necessity to move the frequency extension modules and bend the cables connected to the VNA upon measuring the OMT ports placed in-line or at the right angle, Fig. 9.

It should be noted that the measurements of the cross-pol largely affected by the accuracy of the used interfacing transitions from rectangular-to-square waveguides [12]. Even a very small angular misalignment at the OMT input will generate cross-pol signal and affect the accuracy of the measurements. The rectangular-to-square waveguide transitions used to match the OMT custom-sized waveguide port with the VNA extension modules could be an additional source of the cross-pol signal associated with the waveguide

mode transformation.

The measurements show that the output return loss does not exceed 15 dB but in the major part of the RF band is actually below 20 dB, Fig. 10a. The measured insertion RF loss, Fig. 10b, largely follow the simulation results, Fig. 7b, and are close to 0.45 dB between 250 and 373 GHz while start to worsen below 250 GHz, which is the result of approaching cut off frequency of the waveguide and clearly follows simulation results. With the expected use of the OMT at cryogenic temperature around 4 K, the insertion RF loss should improve down to 0.15 - 0.2 dB with increasing of the gold conductivity at cryogenic temperature. These numbers are based on the measurements performed by authors where Gold conductivity of an electroplated sample was studied in the temperature range 300 - 4 K and resulted in 3 - 4 times improved conductivity at the lowest temperature of 4 K.

The measured cross-pol, Fig. 10c, is better than - 23 dB in all the RF band except for 210 – 220 GHz where the measurements were performed with the frequency extension module WR5.1 and corresponding set of waveguide adapters that match the OMT waveguide dimensions 380 x 760 µm and 760 x 760 µm. The discrepancy in the measured cross-pol in the RF band 210 – 220 GHz could be caused by the adapter used to match the WR5.1 frequency extension module to the OMT square port, which known to be extremely sensitive to the manufacturing tolerances [12]. At all plots, Fig. 10, the features at around 376 GHz are already beyond the target OMT RF operation band and are consequences of the second waveguide mode appearance.

V. Conclusion

We present the design of the orthomode transducer that covers frequency band 210 - 373 GHz with fractional bandwidth up to 56%. The OMT employs a modified Bøifot layout where introduced additional elements help achieving broadband performance. The OMT design features built-in novel 90-degree waveguide twist that allows to minimize length of the H-split internal waveguides and thus minimizes a risk of RF leaks and extra insertion RF losses. Additionally, the twist allows placing the OMT outputs co-aligned that facilitate design of the following receiver components for both polarizations by allowing use the same configuration and components in both polarization chains. The OMT layout makes it suitable to be fitted into a tight space, e.g., of the ALMA receiver cartridge. The OMT was designed and optimized using 3D simulation software and tested with VNA and three VNA extensions [13] in order to cover the ultra-broad RF band. The manufactured prototype performance follows well the simulations. The OMT demonstrated the cross-poll better than 25 dB across 95% of the frequency band with output reflections better than 15 dB and the insertion RF loss better than 0.5 dB. In the Table I, we provide comparison of the different types of published OMTs.

TABLE I
COMPARISON OF STATE-OF-THE-ART OMT

Reference	FBW [%]	Fc [GHz]	RL * [dB]	**IL [dB]	***X-Pol [dB]	Type
[12]	58,1	387,5	17	2.5	35	Bøifot
[14]	26,4	144	20	0.4	30	Bøifot
[15]	49,5	93	15	1	45	Turnstile
[16]	26	442,5	10	2.5	12	Reverse-coupling structure
[17]	25	240	12	0.8	25	Turnstile
[18]	38,8	322,5	15	3	30	Substrate Based
[19]	37,8	92,5	15	0.8	NA	Turnstile
This Work	**55,9**	**291,5**	**15**	**0.8**	**23**	**Bøifot**

FBW: Fractional bandwidth, Fc: Center frequency, NA: Not available. *RL: Return loss, **IL: Insertion loss
***X-Pol. Cross-pol;
The reported values correspond to measurements of the worst-case peak values of both polarizations at RT

An early version of the OMT with external twist was used in SEPIA345 receiver [6] that is installed at APEX telescope in Chile [20] and in operation since January 2020.

Acknowledgments

Authors would like to thank Dr. N. Phillips, ESO, for providing data and original plots on ALMA receivers' beam squint on sky used in Fig. 1.

References

[1] A. M. Bøifot, "Classification of ortho-mode transducers," European Transactions on Telecommunications, vol. 2, no. 5, pp. 503–510, 1991.
[2] ALMA observatory, on-line https://www.almaobservatory.org/
[3] S. Asayama, G. H. Tan, K. Saini, J. Carpenter, G. Siringo, T. Hunter, N. Phillips, H. Nagai, "Report of the ALMA Front-end & Digitizer Requirements Upgrade Working Group", ALMA Report ALMA-05.00.00.00-0048-A-REP
[4] B. Billade et al., "Performance of the First ALMA Band 5 Production Cartridge," in IEEE Transactions on Terahertz Science and Technology, vol. 2, no. 2, pp. 208-214, March 2012, doi: 10.1109/TTHZ.2011.2182220.
[5] V. Belitsky et. al., "ALMA Band 5 receiver cartridge: Design, performance, and commissioning", A&A, A98, Volume 611, March 2018, https://doi.org/10.1051/0004-6361/201731883
[6] D. Meledin, et. al., "SEPIA345: A 345 GHz dual polarization heterodyne receiver channel for SEPIA at the APEX telescope," Astronomy & Astrophysics, 668, A2, 2022, doi: https://doi.org/10.1051/0004-6361/202244211
[7] C. López, V. Desmaris, D. Meledin, A. Pavolotsky, & V. Belitsky, "Design and Implementation of a Compact 90° Waveguide Twist with Machining Tolerant Layout," in IEEE Microwave and Wireless Components Letters, vol. 30, no. 8, pp. 741-744, Aug. 2020, doi: 10.1109/LMWC.2020.3000833
[8] C. López, D. Montofré, V. Desmaris, A. Henkel, & V. Belitsky, "Ultra-Wideband 90° Waveguide Twist for THz Applications," IEEE Transactions on Terahertz Science and Technology, vol. 13, no. 1, pp. 67-73, Jan. 2023, doi: 10.1109/TTHZ.2022.3213468
[9] L. Rud, D. Kulik, A. Kirilenko, "Compact Broadband 90° Twist Based on Square Waveguide Section with Two Stepped Corner Ridges", Microwave and Optical Technology Letters, Vol. 51, No. 3, March 2009, DOI 10.1002/mop
[10] L. Zeng, C. E. Tong, S. N. Paine and P. K. Grimes, "A Compact Machinable 90° Waveguide Twist for Broadband Applications," in IEEE Transactions on Microwave Theory and Techniques, vol. 68, no. 7, pp. 2515-2520, July 2020, doi: 10.1109/TMTT.2020.2987800.
[11] A. Kirilenko, D. Kulik, L. Rud, "Compact 90° Twist Formed by a Double-Corner-Cut Square Waveguide Section", IEEE Transactions on Microwave Theory and Techniques, Vol. 56, No. 7, pp. 1633-1637, July 2008.
[12] A. Gonzalez and K. Kaneko, "High-Performance Wideband Double-Ridged Waveguide OMT for the 275–500 GHz Band," in IEEE Transactions on Terahertz Science and Technology, vol. 11, no. 3, pp. 345-350, May 2021, doi: 10.1109/TTHZ.2021.3062451.
[13] VDI Inc., https://www.vadiodes.com/VDI/pdf/VNA%20Brochure.pdf
[14] S. Asayama and M. Kamikura, "Development of doubled-ridged waveguide orthomode transducer for the 2mm band," J. Infrared Millimeter THz Waves, vol. 30, pp. 573–579, Jun. 2009.

[15]D. Henke and S. Claude, “Design of a 70–116 GHz W-band turnstile OMT,” 2014 44th European Microwave Conference, Rome, Italy, 2014, pp. 456-459, doi: 10.1109/EuMC.2014.6986469.
[16]A. Navarrini, C. Groppi, R. Lin, G. Chattopadhyay, “Test of a Waveguide Orthomode Transducer for the 385-500 GHz Band,” Proc. 22nd Int. Symp. on Space THz Tech., Tucson, 26-28 April 2011.
[17]A. Navarrini, A. Bolatto and R. L. Plambeck, “Test of 1 mm band turnstile junction waveguide orthomode transducer”, Proc. 17th Int. Space Terahertz Technol. Symp., 2006-May-10–12.
[18]N. Patriksson et al., "Novel Orthomode Transducer Scalable to Terahertz Frequencies," 2024 4th URSI Atlantic Radio Science Meeting (AT-RASC), Meloneras, Spain, 2024, pp. 1-4, doi: 10.46620/URSIATRASC24/IPKB8830.
[19]G. Pisano, L. Pietranera, K. Isaak, L. Piccirillo, B. Johnson, B. Maffei, et. al., “A broadband WR10 turnstile junction orthomode transducer,” IEEE Microw. Wireless Compon. Lett., vol. 17, no. 4, pp. 286-288, Apr. 2007.
[20] APEX telescope, on-line https://www.apex-telescope.org/ns/ .

Igor Lapkin received his M.Sc. degree from the Technical State University, Nizhny Novgorod, Russia, in 1985. He currently holds the position of Senior Researcher Engineer at the Group for Advanced Receiver Development, Chalmers University of Technology, Gothenburg, Sweden.

His current interests are designing and developing components, mixers, and heterodyne receivers for radio astronomy. He actively participated in designing the ALMA Band 5 and Band 2 cold cartridge receiver channels and APEX telescope facility instruments, SHeFI and SEPIA.

Cristian Daniel López was born in Buenos Aires, Argentina, in 1990. He received the B.S. degree in electronic engineering from Facultad de Ingeniería del Ejército Grl. Div. Manuel N. Savio, Buenos Aires, Argentina, in 2012, and the M.Sc. degree in microelectronics from Universidad Politecnica de Cataluña, Barcelona, Spain, in 2018.

He received his Ph.D. degree in Electrical Engineering at Chalmers University of Technology, Gothenburg, Sweden in 2024. His current research interests are the design and characterization of cryogenic components for THz systems.

Denis Meledin received a Ph.D. degree in radio-physics from Moscow State Pedagogical University, Moscow, Russia, in 2003. From 2000 to 2003, he was a pre-doctoral fellow with Submillimeter Receiver Lab at Smithsonian Astrophysical Observatory, Cambridge, USA. Since 2003 he has been with the Group for Advanced Receiver Development, Chalmers University of Technology, Gothenburg, Sweden. His work is related to the development of instruments for radio-telescopes (e.g., for ALMA, APEX).

He focuses on designing, developing, and characterization components for radio astronomy receivers operating at microwave and mm/submm wavelengths. Besides that, he is involved in the teaching of B.S and M.S. courses and has been a co-supervisor of a number of Ph.D. students.

Leif Helldner Leif Helldner graduated with advanced diploma in automation technology from Fässberg secondary school, Mölndal, Sweden in 1988, he has been employed at Chalmers University of Technology, Onsala Space Observatory, Onsala, Sweden since 1988, developing, installing and maintaining radiometers, receivers, feeds, telescopes and back-end equipment, for both single-dish and VLBI operation, with deliverables to Onsala Observatory, SEST, APEX, ALMA, LOFAR, SKA, VLBI2010 and more.

Leif became Senior Research Engineer at the Group for Advanced Receiver Development, Gothenburg, Sweden in 2019. His main expertise is mechanical and cryogenic design of radio astronomy receivers, test equipment and components, using mechanical CAD and simulation software for further processing and manufacturing, followed by integration, verification and tests.

Mathias Fredrixon received the B.S. degree in engineering from the Chalmers University of Technology, Gothenburg, Sweden. Since 1998, he has been working at the Group for Advanced Receiver Development, GARD, Onsala Space Observatory, Chalmers University of Technology, Gothenburg, Sweden.

He is currently working as senior research engineer and the main field is mechanical design and development of measuring systems and receivers for radio astronomy. He actively participated in developing ALMA Band 5 and Band 2 receivers, in development and support instruments for the APEX telescope in Chile, in the Swedish Odin satellite and Hershel space telescope projects.

Sven-Erik Ferm started his work as technician in 1995 to participate the Swedish Odin Satellite project at the Chalmers University of Technology, Gothenburg, Sweden. Since 2000, he has been working at the Group for Advanced Receiver Development, GARD, Onsala Space Observatory, Chalmers University of Technology, Gothenburg, Sweden. His experience includes working at camera manufacturer, at Victor Hasselblad, for 15 years. Within the GARD group he is responsible for manufacturing the most fine mechanical parts.

Alexey B. Pavolotsky received the M.S. and Ph.D. degrees from Moscow Aircraft Technology Institute / Technical University, in 1990 and 2003, both in material science and engineering.

Since 2002, he is with the Group for Advanced Receiver Development, Onsala Space Observatory, Chalmers University of Technology, Gothenburg, Sweden. He currently holds a Senior Researcher position. His research interests include low-Tc superconducting thin film processing and characterization, as well as microfabrication in general.

Vincent Desmaris received the M.Sc. degree in material science from the National Institute of Applied Science, Lyon, France, in 1999, and the Ph.D. degree in electrical engineering from the Chalmers University of Technology, Gothenburg, Sweden, in 2006. His thesis concerned the fabrication, characterization, and modeling of AlGaN/GaN microwave transistors.

Since 2006, he has been with the Group for Advanced Receiver Development (GARD), Chalmers University of Technology and currently serves as a Head of GARD. His research interests include the area of terahertz receiver technology, especially microfabrication and characterization of waveguide components and circuits and planar cryogenic microwave devices.

Victor Belitsky (M'95–SM'07) received the M.Sc. degree in electrical engineering from the Moscow Telecommunication Institute in 1977, and the Ph.D. degree in experimental physics from the Institute of Radio Engineering and Electronics, U.S.S.R. Academy of Sciences, Moscow, in 1990.

He is currently Professor at the Group for Advanced Receiver Development, Chalmers University of Technology, Gothenburg, Sweden. His research interests include terahertz and superconducting electronics and components, instrumentation for radio astronomy and environmental science. He was involved in various research and instrumentation projects developing instruments for Onsala Observatory 20 m telescope, ALMA observatory (Band 5 and Band 2), APEX telescope facility instruments (SHeFI and SEPIA).